

Feature aggregation for nutrient deficiency identification in chili based on machine learning

Deffa Rahadiyan^{a,*}, Sri Hartati^{a,*}, Wahyono^a, Andri Prima Nugroho^b

^a Department of Computer Science and Electronics, Universitas Gadjah Mada (UGM), Yogyakarta, Indonesia

^b Department of Agricultural and Biosystems Engineering, Universitas Gadjah Mada (UGM), Yogyakarta, Indonesia

ARTICLE INFO

Article history:

Received 18 July 2022

Received in revised form 5 April 2023

Accepted 25 April 2023

Available online 28 April 2023

Keywords:

Feature Combination

Multi-Layer Perceptron

Classifier

Nutrient deficiency

ABSTRACT

Macronutrient deficiency inhibits the growth and development of chili plants. One of the non-destructive methods that plays a role in processing plant image data based on specific characteristics is computer vision. This study uses 5166 image data after augmentation process for six plant health conditions. But the analysis of one feature cannot represent plant health condition. Therefore, a careful combination of features is required. This study combines three types of features with HSV and RGB for color, GLCM and LBP for texture, and Hu moments and centroid distance for shapes. Each feature and its combination are trained and tested using the same MLP architecture. The combination of RGB, GLCM, Hu moments, and Distance of centroid features results the best performance. In addition, this study compares the MLP architecture used with previous studies such as SVM, Random Forest Technique, Naive Bayes, and CNN. CNN produced the best performance, followed by SVM and MLP, with accuracy reaching 97.76%, 90.55% and 89.70%, respectively. Although MLP has lower accuracy than CNN, the model for identifying plant health conditions has a reasonably good success rate to be applied in a simple agricultural environment.

© 2023 The Authors. Publishing services by Elsevier B.V. on behalf of KeAi Communications Co., Ltd. This is an open access article under the CC BY-NC-ND license (<http://creativecommons.org/licenses/by-nc-nd/4.0/>).

1. Introduction

Lack of macronutrient or micronutrient is one of the causes for the number of chili production being lower than consumption in Indonesia (Bahtiar et al., 2020; Chen and Wang, 2019). Macronutrients include N, P, K, Ca, Mg, S (1000 mg/kg dry matter), and micronutrients include Iron, Mn, Zn, Cu, Cl, B, and Mo (100 mg/kg dry matter) (Wulandhari et al., 2019; Tran et al., 2019). Chili plants that lack macronutrients show visual characteristics on the leaves, such as changes in color, shape, and leaf texture (Taujuddin et al., 2020; Tran et al., 2019; daSilva et al., 2019; N and Saju, 2018; Shah et al., 2018). Nevertheless, identifying nutrient deficiency is difficult for ordinary farmers because several nutrients show similar characteristics (Sinha and Shekhawat, 2020; Watchareeruetai et al., 2018; Harjoko et al., 2019).

Two methods for identifying nutrient deficiencies in plants are destructive and non-destructive. One of the destructive methods is laboratory testing, but the risk of error is more significant due to human error (Harjoko et al., 2019). Digital image processing with machine learning is a non-destructive method that gives more objective results (Kamelia

et al., 2020; Myo Han and Watchareeruetai, 2020). Many studies identify macronutrient deficiencies based on plant images, especially leave images. Several studies used RGB images of leaves of tomatoes, chilies, cucumbers, and others (Bahtiar et al., 2020; Lewis and Espineli, 2020; Jose et al., 2021; Shah et al., 2018). The rule-based method analyzes RGB leaf color information in statistical values, but their model cannot handle high data dimensions (Latte et al., 2017; Latte and Shidnal, 2016; Halim et al., 2021). Several studies have used machine learning to identify macronutrient deficiencies in plants. The Backpropagation-Artificial Neural Network (BP-ANN) model with a diagnostic rate of 97.5%, using hyperspectral image (Shi et al., 2021). In addition, the comparison of K-Nearest Neighbor (KNN) with other methods such as J48, Naive Bayes, Partial Least Square (PLS), Classification and Regression Tree (CART), and Classification Tree (CT). The highest accuracy is 86.52% for the KNN method (Kumar et al., 2015, 2021). Other studies use logistic regression, Support Vector Machine (SVM), and Multi Layer Perceptron (MLP) to identify nutrient deficiency of black gram plants (Rahadiyan et al., 2022a). MLP performs better with 88.33% accuracy than logistic regression and SVM (Myo Han and Watchareeruetai, 2020). Then, another classifier method, such as Naive Bayes and Random Forest Technique (RFT) (Siedliska et al., 2021; Vassallo-Barco et al., 2017). However, the success of the identification model is not only based on the machine learning method used, but also on the combination of features analyzed.

* Corresponding authors.

E-mail addresses: deffa.rahadiyan@mail.ugm.ac.id (D. Rahadiyan), shartati@ugm.ac.id (S. Hartati), wahyo@ugm.ac.id (Wahyono), andrew@ugm.ac.id (A.P. Nugroho).

Several studies have tried to use certain features and their combination to identify macronutrient deficiencies. Research (Drdsh et al., 2021) compares YGB and the percentage of RGB value using ANN, and RGB shows the best accuracy. In addition, HSV and RGB values can be used (Qur'ania et al., 2020; Mashumah et al., 2018). The Gray-Level Co-occurrence matrix (GLCM) method extracts the color and texture information with four different angles (Sosa et al., 2019; Sabri et al., 2020; Vassallo-Barco et al., 2017). Another method for texture is Local Binary Pattern (LBP), but in (Tan et al., 2021)'s study, GLCM is more suitable than LBP for their data. Another extraction method is shape feature extraction using canny and Sobel edge detection (Qur'ania et al., 2020), but research (Lukic et al., 2017) utilizes statistical characteristics of Hu moments from binary leaf image. Not only using one feature, Combining features is important in identifying macronutrient deficiencies (Jeyalakshmi and Radha, 2017; Rahadiyan et al., 2022b). In several researches, the combination of the features improves the result, such as a combination of RGB statistics values and Sobel edge (Wulandhari et al., 2019; Wang et al., 2021b), the combination of GLCM, hue, and color histogram to analyze maize plants (Sabri et al., 2020). Then, the combination of RGB values and texture value of the leaves (Merchant et al., 2018) and the descriptors Blurred Shape Model (BSM) and GLCM to extract shape and texture characteristics in coffee leaves images (Vassallo-Barco et al., 2017). Another study uses K-means Clustering based on texture characteristics with RGB values in the image (Merchant et al., 2018). However, the resulting accuracy is still low due to the limited features used (Yan et al., 2019). However, most studies' feature combinations cannot always improve the accuracy (Qur'ania et al., 2020). The classification model using RGB color extraction produces 70.25% of accuracy, and Sobel edge detection produces 59.52% accuracy (Qur'ania et al., 2020). Nevertheless, the combination of RGB and Sobel edge produces lower accuracy than RGB only. It is about 65.36% of accuracy.

Deep learning, especially Convolutional Neural Network (CNN), is becoming a popular classification method today. However, the CNN method uses an automatic feature extraction feature, so it is challenging to analyze the effect of features combination on the results obtained (Buzzy et al., 2020; Khew et al., 2021). In (Senan et al., 2020), the study compares CNN with other machine learning such as ANN, MLP, and SVM. CNN shows the best result because the convolutional layer learns multi features such as color or texture images (Senan et al., 2020). However, in (Watchareeruetai et al., 2018), CNN produces an accuracy of less than 60% because the deficiency classes have similar characteristics. In another study, (Wang et al., 2021a) performs data augmentation until each class has the same amount of data. Deep learning with an augmentation process increases the accuracy up to 5% (Guerrero et al., 2021; Wang et al., 2021a; Myo Han and Watchareeruetai, 2020). In (Jiang et al., 2020), the study compares the results of processing with segmentation and without segmentation. The result is that image segmentation shows better results than without segmentation.

This study aims to classify six chili plant health conditions using the combination of shape, texture, and color features. Chili in Indonesia is usually grown in an uncontrolled lighting conditions. The use of one feature such as color has a great risk of identification errors because of the lighting condition. So, the proposed study varies several features for nutrient deficiency identification. A careful feature selection was carried out to produce an accurate model that robust in the uncontrolled lighting condition. Some features considered are the leaves' color, shape, and texture. Several other machine learning and deep learning methods, such as MLP, SVM, Naive Bayes, RFT, and CNN were tested to compare the performance models in our data. The contributions of this paper are as follows.

- a. Perform features combination (color, texture, and shape of the chili leaves image) that can be used to identify plant conditions.

- b. Find a suitable MLP architecture based on the combination of these three features.
- c. The data used is in-House dataset.

2. Materials and methods

This study identified six chili plant conditions using digital image processing based on single leaf image data. There are several stages for identification, namely image acquisition, segmentation, image augmentation, feature extraction, and identification tasks. Fig. 1 shows the identification workflow design.

2.1. Leaf data and nutrient status

The initial stage in the identification process is the collection of image data. The dataset used in this case was collected from the hydroponics chili plant in Sleman, Special Region of Yogyakarta, Indonesia. The hydroponics used is a Nutrient Film Technique (NFT) system. The six plant health conditions observed were Healthy, Calcium, Magnesium, Sulfur, Magnesium-Sulfur, and multi-deficiency. The characteristics of each plant's health condition are summarized in Table 1. The initial condition of hydroponic plants is a healthy plant. The data collection scenario is described as follows:

- a Some chili plants suitable to the criteria can grow and develop in an NFT hydroponic system until six weeks after planting. All plants have the same Health condition as shown on Fig. 2(g).
- b This study combines nutrients using various single compound fertilizers according to the criteria for plant needs. Based on (Singh et al., 2019), the need for chili plants in the juvenile phase is shown in Table 2 and Table 3. The reduction of certain single compound fertilizers is calculated to obtain a nutrient solution with a certain macronutrient deficiency.
- c 7 selected plants were sampled in a hydroponic environment by providing macronutrients based on certain levels. The level used in this study consists of 5 levels. Each level is a dose reduction of macronutrient types by 10%, 30%, 50%, 70%, and 90%. The content of these macronutrients is maintained for seven days to observe visible visual characteristics properly.
- d This study validated the data with agricultural experts to ascertain the visual characteristics of the emerging leaves. If appropriate, chili plant data is acquired.
- e The leaf acquired is a single leaf sample that represent the plant's condition.

Visual changes in the leaves are captured using the camera sensor with HD 1080 resolution on a certain background. RGB image camera works like the human eye which is sensitive to RGB light bands. A sample of six classes of data is shown in Fig. 2. The result is obtained many data in specific classes as shown in Table 4, where AAug is data after augmentation and BAug is data before augmentation.

2.2. Preprocessing, segmentation, and augmentation process

This study uses two types of preprocessing to improve image quality. The first is resizing the image to a size of $512 \cdot 512$. While the second is to apply Histogram Equalization (HE) (Abdul et al., 2015). Image acquisition takes place in a natural environment so that the lighting varies. HE is applied to reduce the impact of lighting on the resulting image. Eq. (1) and (2) are formula to do HE, where cdf is a normalization function. Then, intensity transformation of the input image r_k to s_k is where L is the number of possible intensities and n_{rj} is the number of pixels of level r_j .

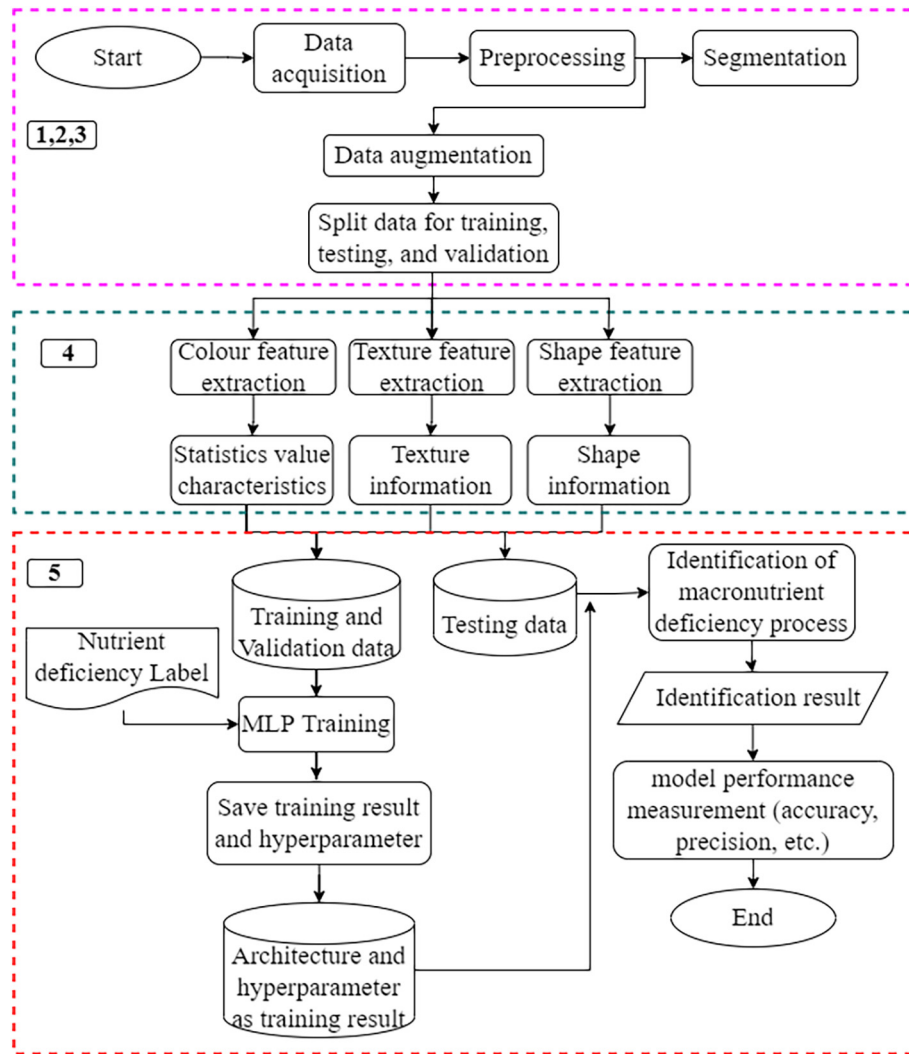


Fig. 1. Stages of identification of macronutrient deficiencies in chili plants.

$$cdf(j) = \sum_{i=0}^k \frac{n_{ij}}{n} \quad (1)$$

$$s_k = T(r_k) = \text{round}(cdf(r_k) \times (L - 1)) \quad (2)$$

Segmentation is the process of separating an object from the background. Histogram equalization results will be segmented to separate objects from complex backgrounds using the thresholding method (Vassallo-Barco et al., 2017). Thresholding is a segmentation method based on certain pixel values. The HE results were converted to a LAB color model in this study. LAB was chosen because it proved suitable

for primary colors, including leaf color. The lower threshold value used is 122 and the upper limit is 245. The a^* channel on the LAB is used. Several morphological operations such as erosion and dilation are used to cover some holes formed. The results of the morphological operations are performed *bitwise not* for the masking process of HE images and binary images.

Data augmentation is a process to multiply data (Guerrero et al., 2021). In several studies, data augmentation has proven to improve the model performance (Guerrero et al., 2021; Kuznichov et al., 2019). The data is reproduced through specific modification processes. In this study, the data augmentation for the training set is executed by several behaviors, namely rotation, shear, zoom, and brightness. Rotation was

Table 1
The visual characteristics of nutrient deficiency.

Plant Condition	Characteristics of the leaves			
	Color	Shape	Texture	Part of the plant
Healthy	Green	Ellipse	Smooth	Overall
(−Ca)	Healthy Green	Misshapen	Curling leaf tip	Top
(−Mg)	Necrosis (cell injury), interveinal chlorosis	Ellipse/ Misshapen	Smooth	Bottom
(−S)	Turning brown on the edge of the leaf	Ellipse/ Misshapen	Smooth/ Curling leaf tip	Bottom
(−MgS)	Necrosis (cell injury), interveinal chlorosis, turning brown on the edge of the leaf	Ellipse/ Misshapen	Smooth/ Curling leaf tip	Bottom
(−Multi)	Multi characteristics	Ellipse/ Misshapen	Smooth/ Curling leaf tip	Top/Bottom

Table 2
Chili plant nutritional requirements.

Compound	PPM	Compound	PPM
%N-NO3	180.0	%Cl	0.0
%N-NH4	7.2	%Fe	1.72
%P2O5	48.0	%B	0.23
%K2O	225.0	%Cu	0.37
%CaO	170.3	%Zn	0.38
%MgO	40.0	%Mn	0.34
%Na	0.0	%Mo	0.06
%SO3	32.5		

chosen because this model is expected to be used in real environments with irregular leaf positions. In addition, *shear* and *zoom* are applied so that the model can cope with the problem of different data acquisition distances. The identification system is designed to be applied to a real environment, so the model must be able to overcome different lighting problems. Therefore, data augmentation also considers brightness behavior. The augmentation data in this study uses Keras tools with a rotational parameter range of 40, a shear range of 0.2, a zoom range of 0.2, and a brightness range of 0.5 to 1.5. Each data is augmented into 8 data. The image resolution was reduced to 500×500 pixels before the augmentation process.

2.3. Feature extraction

The feature extraction helps retrieve information such as color, texture, shape, geometry, and others from the chili leave image. Some studies only analyze one feature, but other studies combine them. This study compares two-color feature extraction methods using statistical value of the RGB and HSV color models. The RGB and HSV leaf color features are helpful features that have been widely used. Color model conversion from RGB to HSV aims to limit the size and type of color space. Then, the texture feature extraction methods compared are LBP and GLCM. The shape feature extraction used is the value of Hu moments and statistical characteristics of the centroid distance in the binary image. Table 5 shows the number of features for each method. The feature combination cannot always improve the performance of the model. Therefore, the selection of features combination must be conducted to obtain an accurate classification.

2.3.1. Color feature extraction

The HSV and RGB color spaces are robust for color extraction features (Latte et al., 2017; Latte and Shidnal, 2016). They analyze the statistical characteristics such as mean, standard deviation, and skewness on each channel in the color model as shown in Eq. (3)–(5). Where μ is Mean, σ is Standard Deviation, *Skewness* is image dimension based i -th pixel, M is the total number of j -th, and N is value of the j -th pixel of the image at the i -th color channel. In (Qur'ania et al., 2020; Drdsh et al., 2021), RGB produces a high accuracy. However, in (Latte et al., 2017) HSV is robust for macronutrient identification. Therefore, this study looks for HSV or RGB feature extraction features that are suitable for our chili plant data. This study extracted the red, green, and blue color component of the RGB image and extracted hue, saturation, and value of the HSV image.

Table 3
Amount of compound requirement for 10 Liters nutrient solution.

Substance name	Formula	Amount (grams)
Magnesium Sulfate	MgSO4, 7H2O	2.5
Calcium Nitrate	5Ca(NO3)2.NH4NO3.10H2O	6.55
Potassium Nitrate	KNO3	5.22
Meroke VITAFLEX	Fe, Mn, Zn, Cu, B, Mo	0.23
Meroke MAP	N, P2O5	1.11
Meroke MKP	P2O5, K2O	0.82

$$\mu = \frac{1}{MN} \sum_{i=1}^M \sum_{j=1}^N (I_{ij}) \quad (3)$$

$$\sigma = \sqrt{\frac{1}{MN} \sum_{i=1}^M \sum_{j=1}^N (I_{ij} - \mu)^2} \quad (4)$$

$$\text{Skewness} = \left(\frac{1}{MN} \sum_{i=1}^M \sum_{j=1}^N ((I_{ij} - \mu)^3) / \sigma^3 \right) \quad (5)$$

2.3.2. Texture feature extraction

The texture is a feature that can be used to identify macronutrient deficiencies. In this study, the class that clearly shows the visual characteristics of the textural features is Calcium. If the research only uses color, then the class labelled Calcium will be challenging to identify because it has color characteristics that are very similar to healthy. In this study, the texture feature extraction method uses two different methods, namely GLCM and LBP. GLCM has been used for texture feature extraction in cases (Sabri et al., 2020; Tan et al., 2021) and give good results. Meanwhile, LBP was tested in case (Kumar et al., 2020).

GLCM is obtained by calculating the probability of the adjacency relationship between two pixels at a certain distance and angle orientation (Widodo et al., 2018). After obtaining the co-occurrence matrix, the observed image's statistical characteristics can be calculated. GLCM statistical features include Contrast, Correlation, ASM, IDM, and Entropy for four angles (0°, 45°, 90°, and 135°) and one distance (1 pixel) as shown in Eq. (6)–(10). Where $GLCM(i, j)$ is the distribution of joint probabilities of a pixel pair, one with gray level i and the other with gray level j . The number of rows and columns of the GLCM matrix depends on the gray level of an image. L is the number of gray levels used minus 1 for computation. The gray level value (grayscale) of an image between 0 and 255. The symbols $\mu'_i, \mu'_j, \sigma'_i, \sigma'_j$ are means and standard deviations of the marginal distributions associated with $GLCM(i, j)$.

$$ASM = \sum_{i=1}^L \sum_{j=1}^L (GLCM(i, j))^2 \quad (6)$$

$$\text{Contrast} = \sum_{n=1}^L n^2 \left\{ \sum_{|i-j|=n} (GLCM(i, j))^2 \right\} \quad (7)$$

$$IDM = \sum_{i=1}^L \sum_{j=1}^L \frac{(GLCM(i, j))^2}{1 + (i - j)^2} \quad (8)$$

$$\text{Entropy} = \sum_{i=1}^L \sum_{j=1}^L (GLCM(i, j) \log (GLCM(i, j))) \quad (9)$$

$$\text{Correlation} = \frac{\sum_{i=1}^L \sum_{j=1}^L (i, j) (GLCM(i, j) - \mu'_i \mu'_j)}{\sigma'_i \sigma'_j}, \text{ where}$$

$$\mu'_i = \sum_{i=1}^L \sum_{j=1}^L i \times GLCM(i, j),$$

$$\mu'_j = \sum_{i=1}^L \sum_{j=1}^L j \times GLCM(i, j),$$

$$\sigma'_i = \sum_{i=1}^L \sum_{j=1}^L GLCM(i, j) (i - \mu'_i)^2$$

$$\sigma'_j = \sum_{i=1}^L \sum_{j=1}^L GLCM(i, j) (j - \mu'_j)^2 \quad (10)$$

LBP is a feature extraction method of binary images. In (Kumar et al., 2020) proves that LBP can solve the problem of rotation on objects according to the data used in this study. For the LBP, we selected the uniform pattern and set the value of bins to 10. Thus, this study extracted

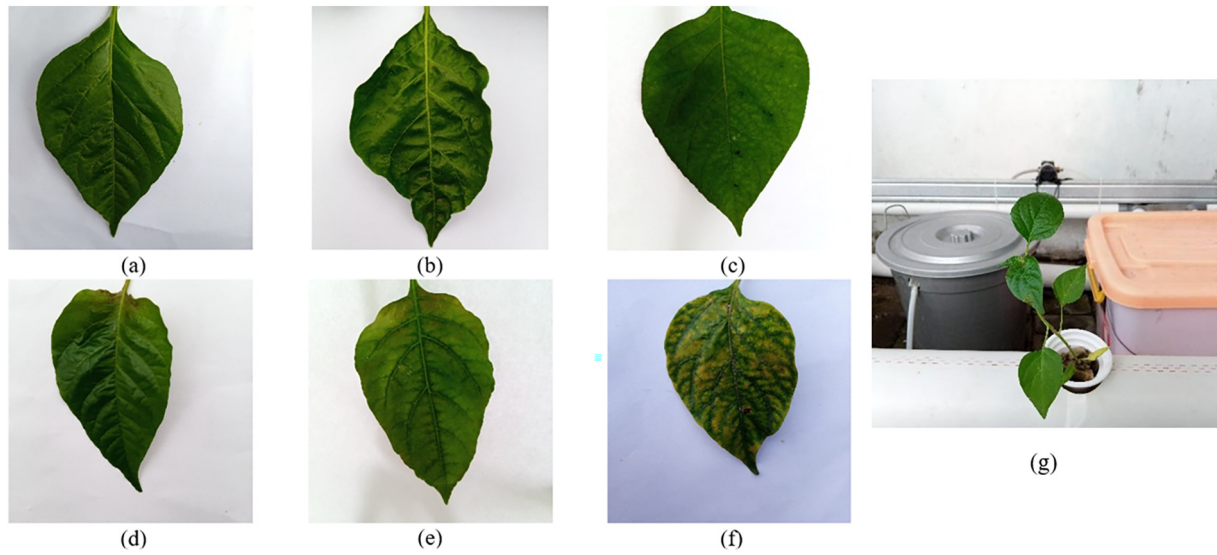


Fig. 2. Sample chili plant leaf images condition, (a) Healthy, (b) Calcium, (c) Magnesium, (d) Sulfur, (e) Magnesium-Sulfur, (f) Multi-deficiency, (g) Hydroponics plant.

ten texture features with the LBP method. The LBP intensity value is calculated for such a specified center pixel gray color by comparing it to its nearest neighbors, as seen in Eq. (11). Where g_c corresponds to the value of the center pixel, g_p to the value of the eight surrounding pixels, P is the total number of involved neighbors, R is the radius of the neighborhood, and function $f_1(x)$.

$$LBP_{P,R} = \sum_{p=0}^{P-1} 2^p \times f_1(g_p - g_c), \quad \text{where} \quad (11)$$

$$f_1(x) = \begin{cases} 1, & x \geq 0 \\ 0, & \text{else} \end{cases}$$

2.3.3. Shape feature extraction

There is a change in leaf shape in plants that lack macronutrients, especially leaf edges. Leaves can be more rounded or even irregular. This study uses the moment to determine the centroid point of an object. The centroid or the center moment of an object is (x', y') shown in Eq. (12), where M_{ij} is x and y coordinate of the i -th location cross the volume of goods moved to or from i -th location.

$$x' = \frac{M_{10}}{M_{00}}, \quad y' = \frac{M_{01}}{M_{00}}, \quad \text{where :} \quad (12)$$

$$M_{ij} = \sum_x \sum_y x^i y^j I(x, y)$$

However, this study presents two different approaches in processing data from the centroid point, such as:

- The centroid point is used to produce moment invariant. Using moment invariants, feature extraction of shape produced

seven-moment invariant values that are not sensitive to translation, scale change, and rotation (Kumar et al., 2020). The seven moment invariant values are shown in Eq. (14)–(20). H_1 is the first moment invariant, H_2 is the second moment invariant, and others, where μ_{ij} in Eq. (13) is means value of distribution $I(x, y)$.

$$\mu_{ij} = \sum_x \sum_y (x-x')^i (y-y')^j I(x, y), \quad \text{where :} \quad (13)$$

$$H_1 = \mu_{20} + \mu_{02} \quad (14)$$

$$H_2 = (\mu_{20} - \mu_{02})^2 + 4\mu_{11}^2 \quad (15)$$

$$H_3 = (\mu_{30} - 3\mu_{12})^2 + 3(\mu_{21} - \mu_{03})^2 \quad (16)$$

$$H_4 = (\mu_{30} + \mu_{12})^2 + (\mu_{21} + \mu_{03})^2 \quad (17)$$

$$H_5 = (\mu_{30} - 3\mu_{12})(\mu_{30} + \mu_{12})[(\mu_{30} + \mu_{12})^2 - 3(\mu_{21} + \mu_{03})^2] \\ (3\mu_{21} - \mu_{03})(\mu_{21} + \mu_{03})[3(\mu_{30} + \mu_{12})^2 - (\mu_{21} + \mu_{03})^2] \quad (18)$$

$$H_6 = (\mu_{20} - \mu_{02})[(\mu_{30} + \mu_{12})^2 - (\mu_{21} + \mu_{03})^2] + 4\mu_{11}(\mu_{30} + 3\mu_{12})(\mu_{21} + \mu_{03}) \quad (19)$$

$$H_7 = (3\mu_{21} - \mu_{03})(\mu_{30} + \mu_{12})[(\mu_{30} + \mu_{12})^2 - 3(\mu_{21} + \mu_{03})^2] - \\ (\mu_{30} - 3\mu_{12})(\mu_{21} + \mu_{03})[3(\mu_{30} + \mu_{12})^2 - (\mu_{21} + \mu_{03})^2] \quad (20)$$

Table 4

Data used in this study.

Plant condition	Total data	Training data		Testing data
		BAug	Aaug	
Healthy (complete nutrient)	98	68	612	30
Calcium (–Ca)	101	71	639	30
Magnesium (–Mg)	100	70	630	30
Sulfur (–S)	96	66	594	30
Magnesium-Sulfur (Mg–S)	102	72	648	30
Multi deficiency (more than 2)	97	67	603	30

Table 5

The number of features.

Type of features	Method	Number of features
Color	HSV Color model	9
	RGB Color model	9
Texture	Statistics feature of GLCM	24
	Local Binary Pattern (LBP)	10
Shape	Hu moments	7
	Distance of centroid	5

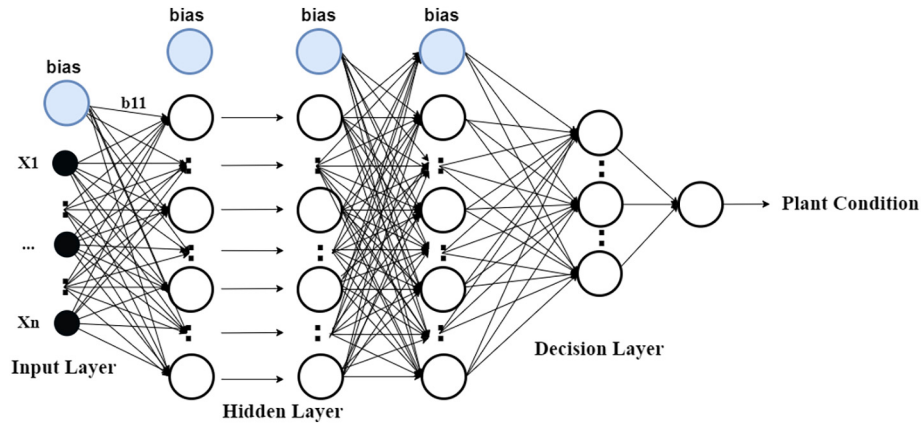


Fig. 3. The multi layer perceptron architecture.

- b. The distance between the centroid and each edge pixel is obtained by calculating the Euclidean distance. Then, the distance is visualized, and the statistical value is sought from the data for each distance to the centroid. The features obtained from this stage are statistical features such as mean, min, max, median, and average.

2.4. Identification model

To classify the six classes of chili plant condition, MLP architecture is used. MLP is an artificial neural network that includes at least three layers of neuron nodes, namely the input layer, the output layer and one or more hidden layers. Except for the input neuron, each node uses a different nonlinear activation than the linear perceptron. Fig. 3 shows the MLP architecture used.

The number of input neurons corresponds to the number of features value used. This study looks for a suitable number of nodes and hidden layers based on the three features combination. In the decision layer, this study uses six nodes which represent six classes of plant health conditions using One-hot encoding output representation. The rectified linear unit (ReLU), is used as the activation function. In mathematical

form, $Y = \phi(wx + b)$, where w is the weight, x denotes as the vectors of input, b is the value of bias and ϕ is the nonlinear activation.

This study uses the MLP architecture model in (Myo Han and Watchareeruetai, 2020) against our data to analyze the combination of three features. In (Myo Han and Watchareeruetai, 2020), the research use two hidden layers with 2048 and 512 nodes. The suitable learning rate is 0.002 with the Adam optimizer. After the best combination of the three features is obtained, this study tries to find the best MLP architecture based on our data. This study varies the number of hidden layers, the number of nodes, the learning rate, and the epochs to produce an accurate model based on a combination of three features, namely color, texture, and leaf shape.

This study also compares the best MLP architecture based on the experiment with other previous work, such as Naive Bayes, RFT, and SVM. Naive Bayes is used on (Vassallo-Barco et al., 2017) with certain parameters, and RFT is used (Sonobe et al., 2020). SVM effectively solves local minima and high dimension problems (Sonobe et al., 2020). SVM has several kernels, and (Xu et al., 2020) uses the Gaussian Radial Basis Function (RBF) kernel. In this method, two hyperparameters, the C regularization parameter and gamma value

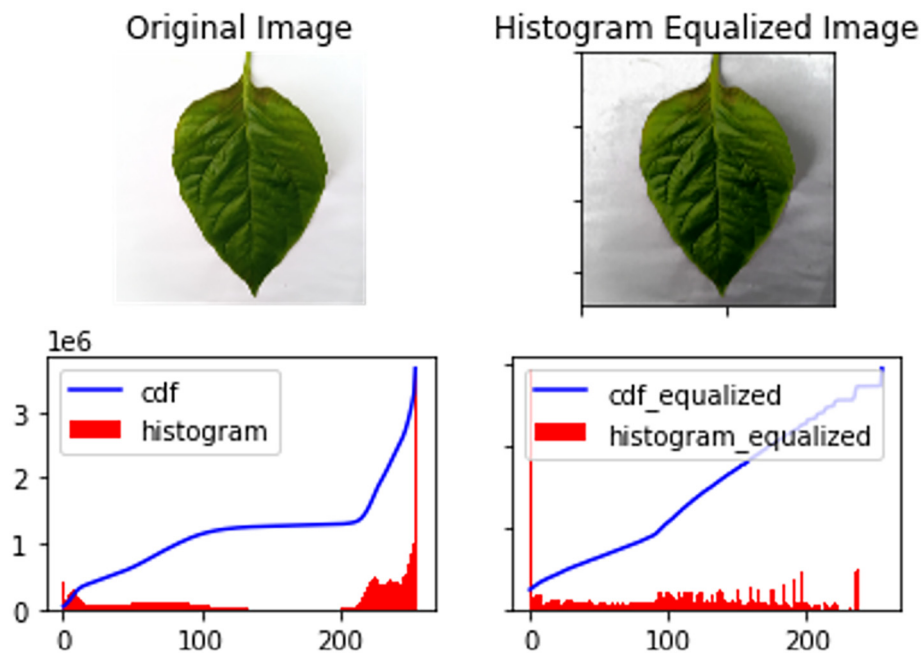


Fig. 4. Comparison of original image and Histogram Equalization result.

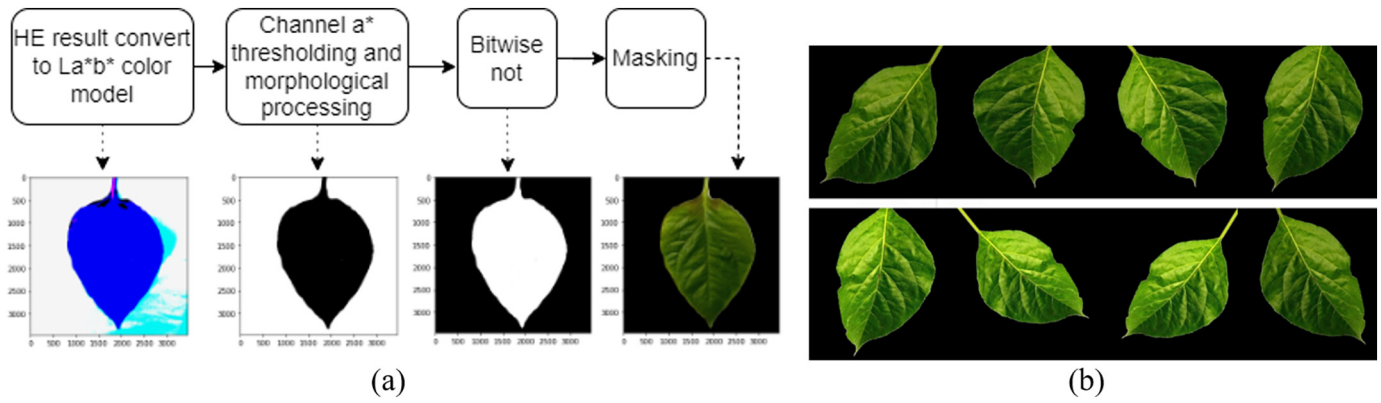


Fig. 5. Result of (a) segmentation, (b) data augmentation process.

are set to generate a classification model. For C, a high score may result in over-fitting due to a high penalty for non-separable points, whereas a low value may result in under-fitting. The value definition of the range of a single training instance of Kernel RBF fits our data with hyperparameter values of gamma of 0.0001, C of 100, and the decision function shape using One vs One classifier (OvO). OvO is used as a multi-class strategy to train models. In addition, this study also tries other SVM kernel such as the Linear kernel (Myo Han and Watchareeruetai, 2020).

2.5. Performance measurement

The parameters used to measure the success of identifying macronutrient deficiencies in plants in this study were accuracy, precision, and recall. The measurement of model performance accuracy is chosen to determine the model's ability to detect all objects correctly. Precision is chosen because several macronutrients exhibit very similar characteristics that the system must distinguish between them. If the system cannot tell the difference, the wrong solution can occur, causing the plant to die. The recall refers to the ratio of correctly predicted positive

observations to all the actual class observations (Xu et al., 2020). The equations used to calculate accuracy, sensitivity, and specificity are shown in Eq. (21) – (23), where *TP* is the number of true positive, *TN* is true negative, *FP* is false positive, and *FN* is false negative.

$$Accuracy = \frac{TP + TN}{TP + TN + FP + FN} \times 100\% \quad (21)$$

$$Precision = \frac{TP}{TP + FP} \times 100\% \quad (22)$$

$$Recall = \frac{TP}{TP + FN} \times 100\% \quad (23)$$

3. Result and discussion

Chili plant data were collected in natural environments, so the lighting condition varied. To fix this problem, this study uses HE. Fig. 4 shows the result of histogram equalization. To separate the object from background, the segmentation process is used. This research uses the

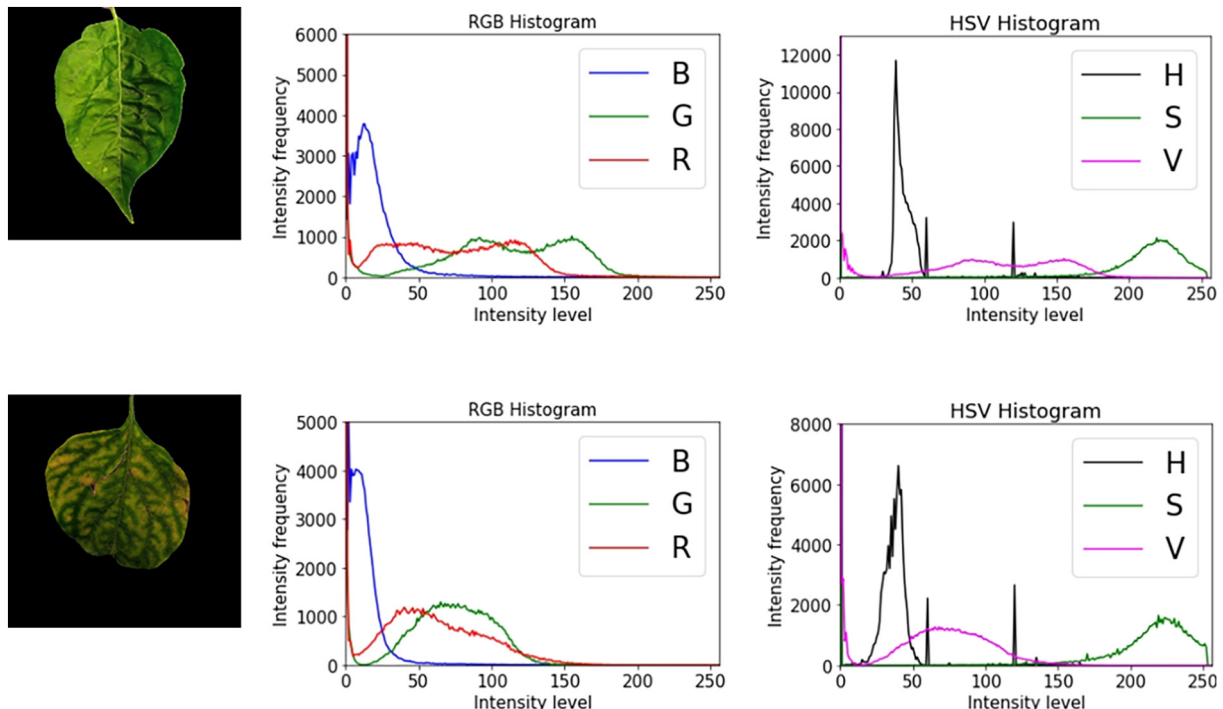


Fig. 6. Histogram of each RGB and HSV color spaces in Calcium and Multi-deficiency data classes.

colorspace segmentation method on channel a^* of the CIELAB image. The approach is to choose a small sample region for each color and to calculate each sample region's average color in a^* space. Based on observations, channel a^* can distinguish object information from the background well, with a range of 122 and 245. However, some noises such as holes can be removed by applied the morphological operations. The result of segmentation is shown in Fig. 5(a). In addition, to increase the model's accuracy, the augmentation process is applied with the results shown by Fig. 5(b).

This study performs a combination of colors, shapes, and textures. For color feature, statistical feature of HSV and RGB are compared. RGB was chosen because research (Qur'ania et al., 2020) is the feature that produces the best performance, while HSV was chosen because in other studies, it can produce the best performance as well. HSV has more complex components to represent object features in more detail. Fig. 6 shows the different characteristics of the two classes. In the green channel of RGB, the Calcium class shows a frequency range from [0, 1400] for intensity level 25 to 185, while unhealthy leaves in the frequency range [0, 1350] for intensity level [10, 135]. In the V channel of the HSV histogram, the peak value for the intensity of the highest frequency of Calcium and Multi-deficiency is around 3000.

This study compares the GLCM and LBP methods for texture feature extraction, while the Hu moments value and the edge distance to the centroid for shape feature extraction. GLCM is a second-order feature extraction where the matrix describes the neighbor relationship between pixels in an image in various directions and local distances. The relationship between class and one of the GLCM features can be seen in Fig. 7. Meanwhile, LBP is a texture extraction feature that is considered invariant to lighting and rotation. The Hu moments value for shape feature extraction consists of seven values that identify the characteristics of a digital image object. These values are independent of translation, rotation, and scaling. At the same time, the other shape extraction feature used is the statistical feature of each edge pixel distance to the centroid. It refers to the visual characteristics of chili leaves that have wavy edges if there is a lack of macronutrient Calcium, multi-deficiency, and others. Therefore, the distance of each leaf edge pixel to the centroid is considered capable of representing the shape features of the leaf. Fig. 8 shows the effect of the pixel distance from the edge to the centroid in different classes. According to Fig. 8 below, healthy exhibits a visual feature that is not smooth/tortuous. This study applies to resizing pixel data into $100 \cdot 100$, so that the distance of each edge pixel point looks far. It causes the visualization to be noisier, coupled with the elliptical leaf shape and tends to be round. Meanwhile, the calcium data shows less noise because the leaf shape is not round.

There are four experimental in this study. The first experiment compares each feature's performance against six chili health condition data classes. The second is the comparison of the feature combination performance. The third experiment compares several MLP hyperparameters against the combination of the three best features obtained from the previous experiment. While the fourth experiment is a comparison of the results of the third experiment with several previous studies.

3.1. Comparison of single feature performance

Before combining features, this study analyzes the abilities of each feature. The MLP architecture in (Myo Han and Watchareeruetai, 2020) is used to determine the features' performance. In addition, this study also analyzes the effect of the data augmentation stage in the resulting identification model. A summary of experiments related to the capabilities of each feature is shown in Table 6.

There are three types of features analyzed: color, texture, and shape features. This study compares the statistical characteristics of RGB and HSV images for color, LBP and GLCM features for textures, and statistical characteristics of the edge pixel distance to centroid and Hu moments for shape characteristics. For color characteristics, the results are in accordance with (Qur'ania et al., 2020) that RGB data in this study produce

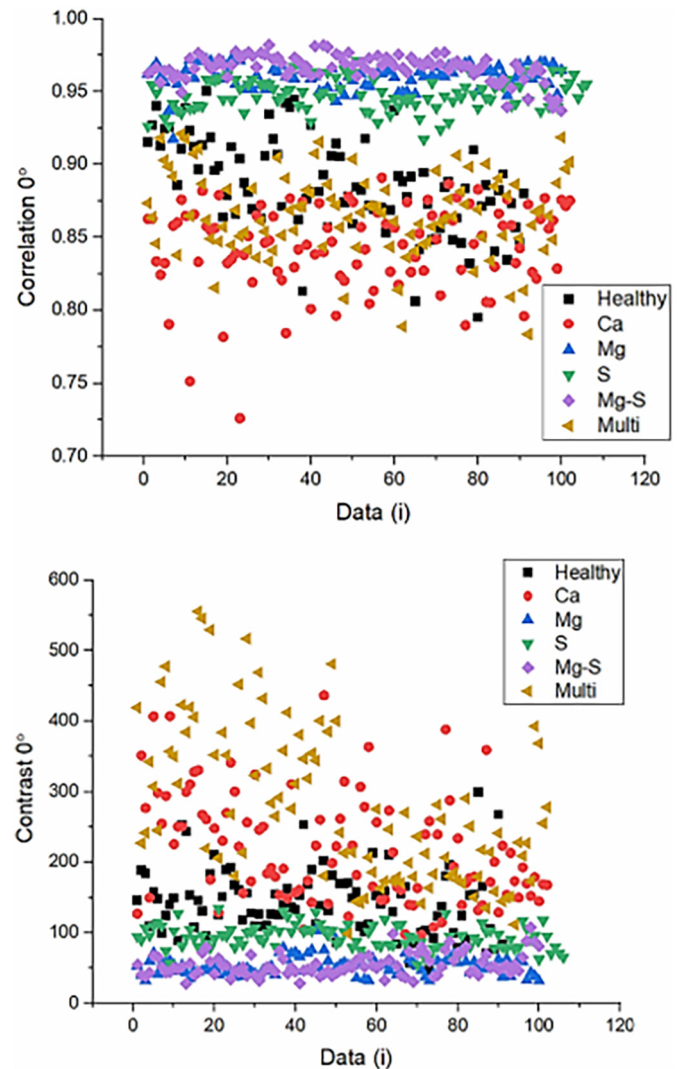


Fig. 7. An example of data visualization in GLCM features.

higher accuracy, precision, and recall values than HSV with an accuracy of 66.28% compared to HSV, which is 49.56%. GLCM produces higher performance than LBP for texture characteristics, which is 50.74%. It is because of LBP describes the texture locally. As for the shape characteristics, statistical characteristics from the edge pixel distance to the centroid resulted in a higher performance of 41.43%.

Furthermore, this study analyzes the augmentation stage's effect on each resulting feature's performance. The result is that augmentation on crop images can increase accuracy by more than 10%, such as RGB features, from 66.28% to 80.00%. This result corresponds with the research (Guerrero et al., 2021; Wang et al., 2021a). After augmentation, RGB and GLCM feature performance remains higher than HSV and LBP. However, different results were obtained on the shape characteristics. The features of Hu moments obtained higher results than the statistical characteristics of the edge pixel distance data set to the centroid. After the augmentation process, features that produce more than 60% accuracy on augmented data are used on a combination of two and three features.

3.2. Comparison of feature combination

The second experiment is to combine different features. The architecture used is MLP by (Myo Han and Watchareeruetai, 2020), same as the previous experiment. Table 7 shows the results of these combinations.

This study performs a combination of two features and three features. A combination of two features is applied to the data before

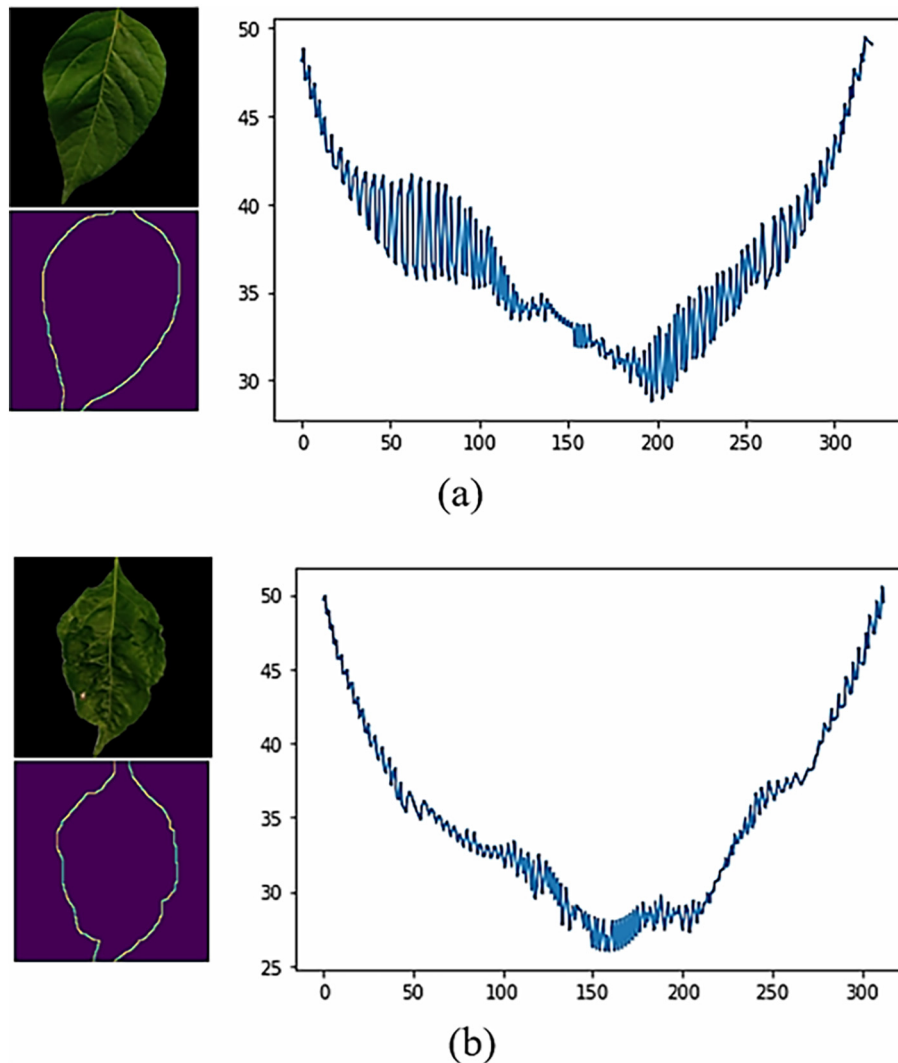


Fig. 8. The distance between edge pixels to the centroid visualization of: (a) Healthy and (b) Ca.

augmentation with a combination of color+texture, color + shape, and texture + shape. The combination of RGB color and GLCM texture produces the highest accuracy, which is 76.13%, compared to the combination of the other two characteristics. In the combination of three features experiment, RGB, GLCM, and Hu moments produces the higher

accuracy than combination of RGB, GLCM, and distance of centroid. This is not in line with the results of previous combinations where the distance of centroid results a higher accuracy than Hu moments feature. In addition, this study also did a combination of 3 features by combining the distance of centroid feature and Hu moments feature. The result was beyond our expectations where the combination accuracy is greater, which is 84.77%.

This study also tries to compare the results of the combination of three data features without augmentation and with augmentation. The result is that data with augmentation yields higher accuracy, according to the previous experiments. The results of the augmentation of the three-feature combination data produce accuracy that is not much different. The combination of RGB, GLCM, and Hu moments produces an accuracy of 86.35%, while RGB, GLCM, and distance of centroid produces an accuracy of 86.21%. But, the combination of RGB, GLCM, Hu, and distance of centroid produced the highest accuracy, which is 87.47%. Because of this, we decided to use this combination in the next experiment.

3.3. Comparison of MLP hyperparameter

This study tries to compare the combination of MLP hyperparameters, such as the number of learning rates and epochs. The number of hidden layers used is three. Based on previous experiments

Table 6
The performance of single feature with augmentation and without augmentation.

	Feature	No.	Method	Total	Accuracy (%)	Precision (%)	Recall (%)
noAug	Color	1	RGB	9	66.28	69.83	65.04
		2	HSV	9	49.56	51.13	49.33
	Texture	3	LBP	10	40.85	43.36	40.45
		4	GLCM	24	50.74	55.43	50.25
	Shape	5	Distance of centroid	5	41.43	54.29	37.68
Aug	Color	6	Hu moments	7	34.84	33.93	33.42
		7	RGB	9	80.00	81.08	81.86
	Texture	8	HSV	9	71.57	72.52	71.35
		9	LBP	10	54.83	58.66	56.36
	Shape	10	GLCM	24	61.38	64.77	63.25
		11	Distance of centroid	5	66.21	64.32	68.14
		12	Hu moments	7	70.53	69.44	71.09

Table 7

The performance of feature combination with augmentation and without augmentation.

	Feature	No.	Method	Total	Accuracy(%)	Precision(%)	Recall(%)
noAug	Color+Texture	1	RGB + GLCM	33	76.13	75.42	73.21
		2	HSV + GLCM	33	72.38	76.10	68.36
	Color+Shape	3	RGB + Hu	16	68.87	72.53	71.33
		4	RGB + Distance of centroid	14	70.29	70.00	70.18
	Texture+Shape	5	GLCM + Hu	31	57.73	51.88	60.25
		6	GLCM + Distance of centroid	29	63.12	67.35	65.23
	Color+Texture+Shape	7	RGB + GLCM + Hu	40	83.27	83.14	81.32
		8	RGB + GLCM + Centroid	38	78.26	72.63	77.32
		9	HSV + GLCM + Hu	40	74.14	68.39	71.43
		10	HSV + GLCM + Centroid	38	78.26	72.63	77.32
		11	RGB + GLCM + Hu + Centroid	45	84.77	85.21	84.62
Aug	Color+Texture	1	RGB + GLCM	33	80.04	85.48	82.36
		2	HSV + GLCM	33	80.75	82.84	81.28
	Color+Shape	3	RGB + Hu	16	82.73	83.13	83.87
		4	RGB + Distance of centroid	14	77.85	78.05	76.57
		3	HSV + Hu	16	65.80	70.64	65.76
	Texture+Shape	4	HSV + Distance of centroid	14	70.65	69.93	70.23
		5	GLCM + Hu	31	62.46	66.25	64.81
		6	GLCM + Distance of centroid	29	70.58	71.66	70.41
	Color+Texture+Shape	7	RGB + GLCM + Hu	40	86.35	88.14	86.52
		8	RGB + GLCM + Centroid	38	86.21	87.67	84.93
		9	RGB + GLCM + Hu + Centroid	40	87.47	88.93	87.16

as shown on Table 8, the number of nodes are 2048, 1024, and 512. The result of hyperparameter shows on Table 9.

The third experiment was carried out by varying the learning rate value from 2 to 0.0001 with a fixed epoch value of 200. The value of 0.0001 was chosen because the resulting performance trend decreased at that value. Based on the experimental results, the highest performance was produced by a learning rate of 0.002, with each accuracy, precision, and recall value of 89.70%, 90.62%, and 89.17%. In comparison, the lowest performance is generated by the learning rate with a value of 2. In training using the Adam optimizer, the learning rate value regulates the number of updates made to the weight value of w . If the learning rate value is decrease, the error function will decrease. However, a learning rate that is too small can cause the performance of training model decreases, as shown by the experiment. After obtaining the appropriate learning rate, this study also looks for the appropriate epoch value based on the previous MLP architecture. The epoch value varied from 100 to 400. The epochs value stopped varying at 400 because the performance trend had declined at that number. Based on the

experimental results, the highest model performance is produced by the MLP architecture with an epoch value of 300. The resulting accuracy, precision, and recall values are 89.70%, 90.62%, and 89.17%, respectively. The greater the iteration value, the more learning is generated. However, an epoch value that is too large can result in an overfitting model. Therefore, the correct learning rate and epoch values must be obtained so that the resulting model performs well.

3.4. Comparison of the MLP in this study with previous study

In the fourth experiment, this study compares the combination of three features with several types of classifiers. For the MLP method, this study compares the architecture in (Myo Han and Watchareeruetai, 2020) in the existing data with the best MLP architecture based on this study. The MLP architecture in this study uses three hidden layers with 2048, 1024, and 512 nodes respectively and an output layer with three nodes. The architecture uses Rectified Linear Unit (ReLU) as an activation function and 300 for epochs. This study uses the cross-entropy category as a loss function because the problem is multi-classification. The study uses Adam as solver (Shi et al., 2019), with a learning rate of 0.002. The result is that the (Myo Han and Watchareeruetai, 2020) architecture produces a relatively high accuracy of 87.47%, but the MLP architecture in this study produces a greater accuracy of 89.18%. In addition, this study compares two SVM kernels: the RBF kernel and the linear kernel. Where C is 1 and γ is 1, the linear kernel can produce an accuracy of 90.55%. In

Table 8

The number of hidden layer and node experiment.

HL1	HL2	HL3	Accuracy(%)	Precision(%)	Recall(%)
4096	–	–	85.50	85.93	86.11
2048	–	–	83.74	84.97	84.64
1024	–	–	81.43	83.88	82.32
512	–	–	80.87	82.62	81.04
256	–	–	80.25	82.19	80.83
128	–	–	73.73	77.10	74.48
4096	4096	–	82.17	84.62	83.86
2048	2048	–	86.58	87.37	87.97
2048	1024	–	84.94	86.80	84.54
2048	512	–	84.32	85.75	85.39
2048	256	–	84.83	85.45	84.61
2048	128	–	79.27	81.49	80.55
2048	2048	2048	78.48	80.33	78.18
2048	2048	1024	86.26	87.40	86.62
2048	2048	512	85.60	86.81	85.28
2048	2048	256	84.78	84.43	84.20
2048	1024	1024	85.52	87.26	85.29
2048	1024	512	87.42	88.70	87.98
2048	1024	256	85.14	87.21	85.37
2048	512	512	86.08	87.37	86.24
2048	512	256	82.84	84.49	83.63
2048	256	256	85.15	86.72	85.46
2048	256	128	80.71	84.06	82.58

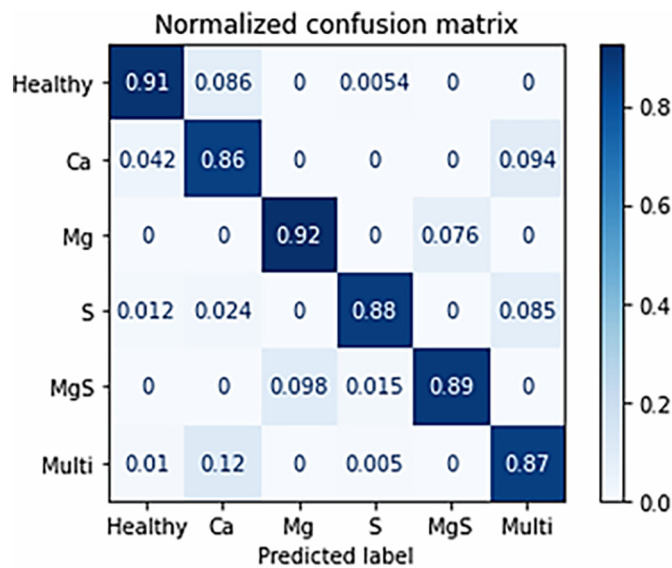
Table 9

Tuning hyperparameter in MLP architecture.

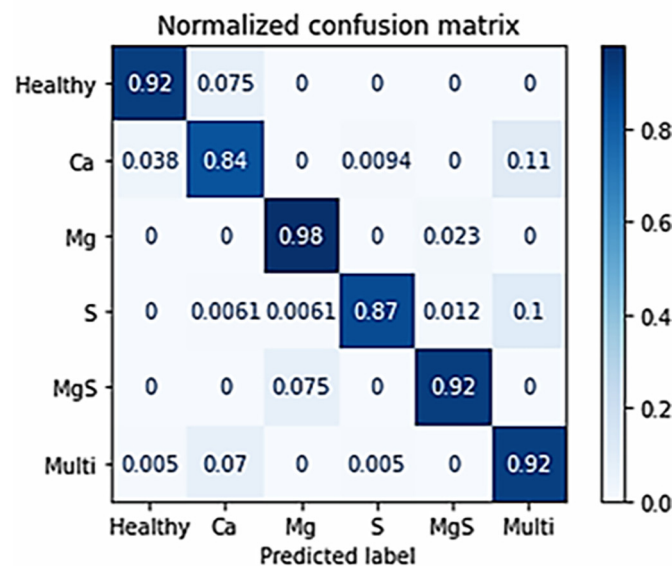
LR	Epochs	Accuracy(%)	Precision(%)	Recall(%)
2	200	20.72	23.12	17.20
2	200	21.13	18.10	17.47
0.1	200	33.25	20.54	27.65
0.05	200	35.81	33.26	34.16
0.001	200	86.74	88.86	86.93
0.002	200	87.91	88.12	88.33
0.003	200	82.26	84.57	83.10
0.005	200	81.72	84.13	83.27
0.0001	200	77.83	82.80	76.54
0.002	100	86.11	88.45	87.32
0.002	250	87.34	88.39	87.76
0.002	300	89.70	90.62	89.17
0.002	350	87.25	88.14	87.32
0.002	400	85.85	86.77	85.81

contrast, the RBF kernel requires parameter tuning with a significant value to produce high accuracy, 100 for C and the gamma value of 0.001. The linear kernel separates the data based on a firm line. Then, SVM can handle non-linear data based on the kernel. This is in accordance with the results of experiments in research (N and Saju, 2018). Besides MLP and SVM, this study also tries to compare other classifiers, such as Naive Bayes and RFT, but their accuracy is not higher than SVM and MLP. This study also compares machine learning methods with CNN (Cevallos et al., 2020). CNN produces the highest accuracy, which is equal to 97.76%. However, CNN has a higher complexity than MLP. The confusion matrix of the proposed MLP architecture and linear SVM kernel is shown in Fig. 9(a) and Fig. 9(b). While the training and validation graphs from CNN are shown in the Fig. 10. The performance comparison shown on Table 10.

The highest overall accuracy is generated by the CNN method, while the second is the SVM linear kernel, and the third is MLP. SVM produces

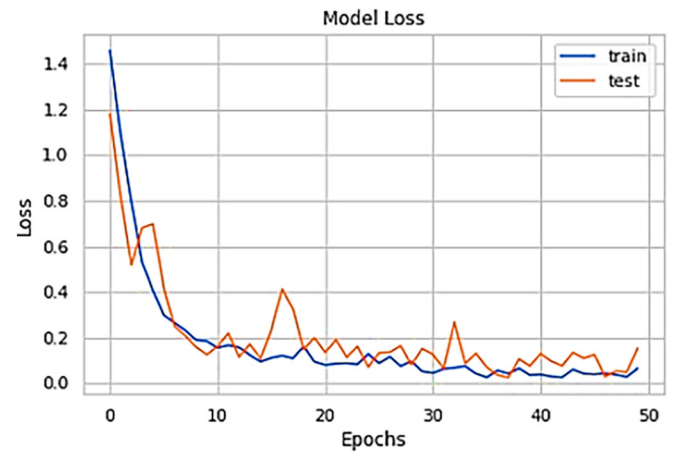


(a)

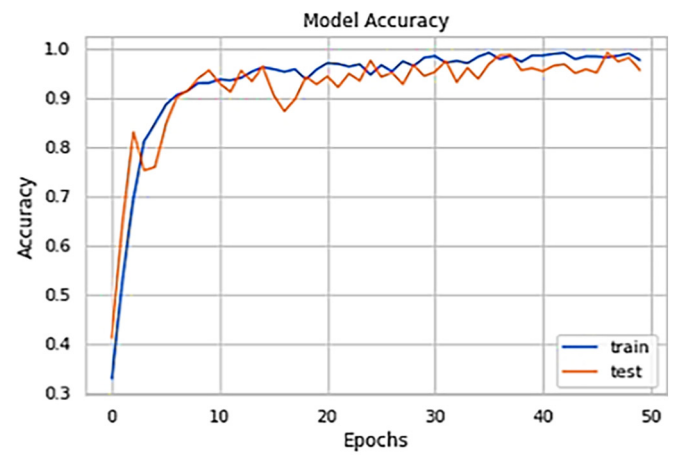


(b)

Fig. 9. Confusion matrix of nutrient deficiency identification using The MLP and SVM.



(a)



(b)

Fig. 10. CNN result.

higher accuracy in detecting Mg, S, Mg—S, and Multi-deficiency classes. However, the MLP architecture in this study yielded higher precision for Healthy and Ca classes. Example of testing data against to the proposed method show on Fig. 11. Even though it is lower, the training time required for MLP is relatively less compared to CNN and SVM linear kernel. It is caused by optimize the C regularization and parameter which means that performing a grid search will usually take more time in SVM.

Several cases cannot be adequately identified in the macronutrient deficiency identification system. The first is healthy, Calcium, and Sulfur. For Calcium, the lack of macronutrient at low levels only gave a slight impact in the form of differences in texture, while sulfur at low levels

Table 10
Comparison of accuracy, precision, and recall with a previous work.

Feature	Method	Accuracy (%)	Precision (%)	Recall (%)
RGB + GLCM + Hu moments+ Distance of centroid	MLP [26]	87.47	88.93	87.16
	MLP (Results of this study)	89.70	90.62	89.17
	SVM (Linear kernel) [26]	90.55	90.34	89.90
	SVM (RBF kernel) [50]	82.37	84.58	83.82
	Naive Bayes [44]	70.66	68.72	70.16
	RFT [36]	63.25	64.33	64.65
Automatic feature extraction	CNN [4]	97.76	93.21	96.95













Data	Predict Class	Actual Class	Data	Predict Class	Actual Class
	Calcium	Calcium		Multidef	Calcium
	Calcium	Mg-S		Mg	Mg
	Multidef	Multidef		Healthy	Mg
	Healthy	Healthy		Sulfur	Mg-S
	Healthy	Healthy		Mg-S	Mg-S
	Multidef	Multidef		Sulfur	Sulfur

Fig. 11. Examples of some test data results against proposed models.

only gave a black color change at the base of the leaves. Therefore, even though a combination of 3 characteristics has been carried out, the developed model can still give incorrect identification results. In addition, there are conditions of overlapping characteristics such as Mg, S, and Mg—S. So, the identification model cannot recognize them correctly in certain cases, especially if the Mg—S is still at a low level.

4. Conclusion

Determining nutrient deficiencies in chili plants can be done using machine learning and deep learning approaches. This study compares the combination of several features. The combination of the leaves color, texture, and shape has been proven to increase the model's accuracy. The best feature combination is generated by RGB, GLCM, Hu, and distance of centroid. The features combined in the augmented data results produce the best performance using a 0.002 of learning rate and 300 epochs with 89.70% of accuracy. This study compares the MLP architecture with several machine learning in the previous study. The result is that SVM produces the best performance with 90.55% of accuracy. Although SVM linear kernel produces higher accuracy than MLP, MLP in this study still has a high success rate. So it can be concluded that the two models can be recommended to identify plant health conditions. MLP in this study proved to be better at identifying plant conditions in the form of Calcium and Sulfur than linear SVM kernels. In addition,

augmented data has been shown to improve accuracy by more than 3%. In addition, this study also compares machine learning with deep learning, such as CNN. CNN is proven to produce higher performance compared to machine learning. However, CNN has a high complexity compared to ordinary machine learning. The model for identifying plant health conditions can be applied to the agricultural environment. One example is the intelligent hydroponic farming system. In addition to monitoring and controlling agricultural environmental conditions, farmers can also embed our model to monitor plant health regularly and provide nutrient solutions based on plant conditions. To support precision agriculture, we will focus on a model that can identify the type of macronutrient deficiency and estimate the percentage of deficiency in the future.

CRedit authorship contribution statement

Deffa Rahadiyan: Conceptualization, Methodology, Software, Validation, Formal analysis, Investigation, Writing – original draft, Writing – review & editing, Visualization. **Sri Hartati:** Conceptualization, Methodology, Validation, Writing – review & editing, Formal analysis, Investigation, Visualization, Supervision, Project administration. **Wahyono:** Conceptualization, Methodology, Validation, Writing – review & editing, Visualization, Project administration. **Andri Prima Nugroho:** Conceptualization, Methodology, Validation, Writing – review & editing, Visualization.

Declaration of Competing Interest

The authors declare that they have no known competing financial interests or personal relationships that could have appeared to influence the work reported in this paper.

Acknowledgements

This research was funded by the Directorate of Research and Community Service, Deputy for Strengthening Research and Development, Ministry of Research, Technology/National Research and Innovation Agency of the Republic of Indonesia in the PMDSU program with grant ID 018/E5/PG.02.00. PT/2022 and 1773/UN1/DITLIT/Dit -Lit/PT.01.03/2022.

References

- Abdul, M., Radhi, H., Musa, A., Al-Hsnue, O., 2015. Enhancement of the captured images under different lighting conditions using histogram equalization method. *Intern. J. Latest Res. Sci. Technol.* ISSN 3, 25–28.
- Bahtiar, A.R., Pranowo Santoso, A.J., Juhariah, J., 2020. Deep learning detected nutrient deficiency in chili plant. 2020 8th International Conference on Information and Communication Technology (ICoICT), pp. 1–4. <https://doi.org/10.1109/ICoICT49345.2020.9166224>.
- Buzzy, M., Thesma, V., Davoodi, M., Velni, J.M., 2020. Real-time plant leaf counting using deep object detection networks. *Sensors (Switzerland)* 20, 1–14. <https://doi.org/10.3390/s20236896>.
- Cevallos, C., Ponce, H., Moya-Albor, E., Brieva, J., 2020. Vision-based analysis on leaves of tomato crops for classifying nutrient deficiency using convolutional neural networks. 2020 International Joint Conference on Neural Networks (IJCNN), pp. 1–7. <https://doi.org/10.1109/IJCNN48605.2020.9207615>.
- Chen, Z., Wang, X., 2019. Model for estimation of total nitrogen content in sandalwood leaves based on nonlinear mixed effects and dummy variables using multispectral images. *Chemom. Intell. Lab. Syst.* 195, 103874. <https://doi.org/10.1016/j.chemolab.2019.103874>.
- daSilva, M.P.S., Mendonc Freitas, M.S., CesarSantos, P., de Carvalho, A.J.C., Jorge, T.S., 2019. Capsicum annum var. annum under macronutrients and boron deficiencies: leaf content and visual symptoms. *J. Plant Nutr.* 42, 417–427. <https://doi.org/10.1080/01904167.2018.1544255>.
- Drdsh, J., Eleyan, D., Eleyan, A., 2021. A prediction olive diseases using machine learning models, decision tree and Naïve Bayes models. *J. Theor. Appl. Inf. Technol.* 99, 4231–4240.
- Guerrero, R., Renteros, B., Castañeda, R., Villanueva, A., Belupú, I., 2021. Detection of nutrient deficiencies in banana plants using deep learning. 2021 IEEE International Conference on Automation/XXIV Congress of the Chilean Association of Automatic Control (ICA-ACCA), pp. 1–7. <https://doi.org/10.1109/ICAACCA51523.2021.9465311>.
- Halim, N.H.N.A., Husin, Z.H., Qadir, T.O., 2021. Brown spot disease severity level detection using binary-RGB image masking. (IJACSA). *Int. J. Adv. Comput. Sci. Appl.* 12, 548–553. <https://doi.org/10.14569/IJACSA.2021.0120962>.
- Harjoko, A., Prahara, A., Supardi, T.W., Candradewi, I., Pulungan, R., Hartati, S., 2019. Image processing approach for grading tobacco leaf based on color and quality. *Intern. J. Smart Sens. Intell. Syst.* 12, 1–10. <https://doi.org/10.21307/ijssis-2019-010>.
- Jeyalakshmi, S., Radha, R., 2017. A review on diagnosis of nutrient deficiency symptoms in plant leaf image using digital image processing. *ICTACT J. Image Video Proces.* 7, 1515–1524. <https://doi.org/10.21917/ijvip.2017.0216>.
- Jiang, F., Lu, Y., Chen, Y., Cai, D., Li, G., 2020. Image recognition of four rice leaf diseases based on deep learning and support vector machine. *Comput. Electron. Agric.* 179, 105824. <https://doi.org/10.1016/j.compag.2020.105824>.
- Jose, A., Nandagopalan, S., Ubalanka, V., Viswanath, D., 2021. Detection and classification of nutrient deficiencies in plants using machine learning. *J. Phys. Conf. Ser.* 1850, 012050. <https://doi.org/10.1088/1742-6596/1850/1/012050>.
- Kamelia, I., Rahman, T.K.B.A., Saragih, H., Haerani, R., 2020. The comprehensive review on detection of macro nutrients deficiency in plants based on the image processing technique. *Proceedings - 2020 6th International Conference on Wireless and Telematics, ICWT 2020*, pp. 7–10. <https://doi.org/10.1109/ICWT50448.2020.9243623>.
- Kheew, C.Y., Teow, Y.Q., Lau, E.T., Hwang, S.S., Bong, C.H., Lee, N.K., 2021. Evaluation of deep learning for image-based black pepper disease and nutrient deficiency classification. 2021 2nd International Conference on Artificial Intelligence and Data Sciences (AiDAS), pp. 1–6. <https://doi.org/10.1109/AiDAS53897.2021.9574346>.
- Kumar, A., Patidar, V., Khazanachi, D., Saini, P., 2015. An approach to improve classification accuracy of leaf images using dorsal and ventral features. *Int. J. Adv. Comput. Sci. Appl.* 6, 9. <https://doi.org/10.14569/ijacsa.2015.060917>.
- Kumar, S., A.G.T., Sreekumar, K., 2020. Classification of rice leaf spot disease using local binary patterns. *Intern. J. Innov. Technol. Expl. Eng.* 9, 510–512. <https://doi.org/10.35940/ijitee.I3866.049620>.
- Kumar, S., Jain, A., Shukla, A.P., Singh, S., Raja, R., Rani, S., Harshitha, G., Alzain, M.A., Masud, M., 2021. A comparative analysis of machine learning algorithms for detection of organic and nonorganic cotton diseases. *Math. Probl. Eng.* 2021. <https://doi.org/10.1155/2021/1790171>.
- Kuznitschov, D., Zvirin, A., Honen, Y., Kimmel, R., 2019. Data augmentation for leaf segmentation and counting tasks in rosette plants. *IEEE/CVF Conference on Computer Vision and Pattern Recognition Workshops (CVPRW)*, Long Beach, CA, USA, 2019, pp. 2580–2589. doi: 10.1109/CVPRW.2019.00314.
- Latte, M.V., Shidnal, S., 2016. Multiple nutrient deficiency detection in paddy leaf images using color and pattern analysis. *International Conference on Communication and Signal Processing, ICCSP 2016*, pp. 1247–1250. <https://doi.org/10.1109/ICCSP.2016.7754352>.
- Latte, M.V., Shidnal, S., Anami, B.S., 2017. Rule based approach to determine nutrient deficiency in Paddy leaf images. *Intern. J. Agric. Technol.* 13, 227–245.
- Lewis, K.P., Espineli, J.D., 2020. Classification and detection of nutritional deficiencies in coffee plants using image processing and convolutional neural network (Cnn). *Int. J. Sci. Technol. Res.* 9, 2076–2081.
- Lukic, M., Tuba, E., Tuba, M., 2017. Leaf recognition algorithm using support vector machine with Hu moments and local binary patterns. *SAMI 2017 - IEEE 15th International Symposium on Applied Machine Intelligence and Informatics, Proceedings*, pp. 485–490. <https://doi.org/10.1109/SAMI.2017.7880358>.
- Mashumah, S., Rivai, M., Irfansyah, A.N., 2018. Nutrient Film Technique based Hydroponic System Using Fuzzy Logic Control. *Proceeding - 2018 International Seminar on Intelligent Technology and Its Application*. 2018. ISITIA, pp. 387–390. <https://doi.org/10.1109/ISITIA.2018.8711201>.
- Merchant, M., Paradkar, V., Khanna, M., Gokhale, S., 2018. Mango Leaf Deficiency Detection Using Digital Image Processing and Machine Learning. 2018 3rd International Conference for Convergence in Technology, I2CT 2018, pp. 1–3. <https://doi.org/10.1109/I2CT.2018.8529755>.
- Myo Han, K.A., Watchareeruetai, U., 2020. Black gram plant nutrient deficiency classification in combined images using convolutional neural network. 2020 8th International Electrical Engineering Congress, IEEECON 2020. <https://doi.org/10.1109/IEEECON48109.2020.2295662>.
- N, L., Saju, K.K., 2018. Classification of macronutrient deficiencies in maize plant using machine learning. *Intern. J. Elect. Comput. Eng. (IJECE)* 8, 4197–4203. <https://doi.org/10.11591/ijece.v8i6.pp4197-4203>.
- Qur'ania, A., Harsani, P., Triastinurmatiningsih, T., Wulandhari, L.A., Gunawan, A.A.S., 2020. Color extraction and edge detection of nutrient deficiencies in cucumber leaves using artificial neural networks. *CommIT (Commun. Inform. Technol.)* J. 14, 23. <https://doi.org/10.21512/commit.v14i1.5952>.
- Rahadiyan, D., Hartati, S., Wahyono, Nugroho, A.P., 2022a. An overview of identification and estimation nutrient on plant leaves image using machine learning. *J. Theor. Appl. Inf. Technol.* 100.
- Rahadiyan, D., Hartati, S., Wahyono, Nugroho, A.P., 2022b. Design of an intelligent hydroponics system to identify macronutrient deficiencies in chili. *Int. J. Adv. Comput. Sci. Appl.* 13. <https://doi.org/10.14569/IJACSA.2022.0130117>.
- Sabri, N., Kassim, N.S., Ibrahim, S., Roslan, R., Mangshor, N.N.A., Ibrahim, Z., 2020. Nutrient deficiency detection in maize (*Zea mays* L.) leaves using image processing. *IAES Intern. J. Artif. Intell.* 9, 304–309. <https://doi.org/10.11591/ijai.v9.i2.pp304-309>.
- Senan, N., Aamir, M., Ibrahim, R., Taujuddin, N.S., Muda, W.H., 2020. An efficient convolutional neural network for paddy leaf disease and pest classification. *Int. J. Adv. Comput. Sci. Appl.* 11, 116–122. <https://doi.org/10.14569/IJACSA.2020.0110716>.
- Shah, A., Gupta, P., Ajgar, Y.M., 2018. Macro-Nutrient Deficiency Identification in Plants Using Image Processing and Machine Learning. 2018 3rd International Conference for Convergence in Technology, I2CT 2018, pp. 1–4. <https://doi.org/10.1109/I2CT.2018.8529789>.
- Shi, J., Wang, Y., Li, Z., Huang, X., Shen, T., Zou, X., 2021. Characterization of invisible symptoms caused by early phosphorus deficiency in cucumber plants using near-infrared hyperspectral imaging technology. *Spectrochim. Acta A Mol. Biomol. Spectrosc.*, 120540. <https://doi.org/10.1016/j.saa.2021.120540>.
- Shi, W., van de Zedde, R., Jiang, H., Kootstra, G., 2019. Plant-part segmentation using deep learning and multi-view vision. *Biosyst. Eng.* 187, 81–95. <https://doi.org/10.1016/j.biosystemseng.2019.08.014>.
- Siedliska, A., Baranowski, P., Pastuszka-Woźniak, J., Zubik, M., Krzyszczyk, J., 2021. Identification of plant leaf phosphorus content at different growth stages based on hyperspectral reflectance. *BMC Plant Biol.* 21, 1–17. <https://doi.org/10.1186/s12870-020-02807-4>.
- Singh, H., Dunn, B.L., Payton, M., Brandenberger, L., 2019. Selection of fertilizer and cultivar of sweet pepper and eggplant for hydroponic production. *agronomy* 433, 1–11. <https://doi.org/10.3390/rs12193265>.
- Sinha, A., Shekhawat, R.S., 2020. Olive spot disease detection and classification using analysis of leaf image textures. *Proc. Comp. Sci.* 167, 2328–2336. <https://doi.org/10.1016/j.procs.2020.03.285>.
- Sonobe, R., Yamashita, H., Mihara, H., Morita, A., Ikka, T., 2020. Estimation of leaf chlorophyll a, b and carotenoid contents and their ratios using hyperspectral reflectance. *Remote Sens.* 12, 1–19. <https://doi.org/10.3390/agronomy9080433>.
- Sosa, J., Ramírez, J., Vives, L., Kemper, G., 2019. An algorithm for detection of nutritional deficiencies from digital images of coffee leaves based on descriptors and neural networks. 2019 22nd Symposium on Image, Signal Processing and Artificial Vision, STSIVA 2019 - Conference Proceedings, pp. 3–7. <https://doi.org/10.1109/STSIVA.2019.8730286>.
- Tan, L., Lu, J., Jiang, H., 2021. Tomato leaf diseases classification based on leaf images: a comparison between classical machine learning and deep learning methods. *AgriEngineering* 3, 542–558. <https://doi.org/10.3390/agriengineering3030035>.
- Taujuddin, N.S., Mazlan, A.I., Ibrahim, R., Sari, S., Ghani, A.R., Senan, N., Muda, W.H., 2020. Detection of plant disease on leaves using blobs detection and statistical analysis. *Int. J. Adv. Comput. Sci. Appl.* 11, 407–411. <https://doi.org/10.14569/IJACSA.2020.0110852>.
- Tran, T.T., Choi, J.W., Le, T.T.H., Kim, J.W., 2019. A comparative study of deep CNN in forecasting and classifying the macronutrient deficiencies on development of tomato plant. *Appl. Sci. (Switzerland)* 9, 14569. <https://doi.org/10.3390/app9081601>.

- Vassallo-Barco, M., Vives-Garnique, L., Tuesta-Monteza, V., Mejía-Cabrera, H.I., Toledo, R.Y., 2017. Automatic detection of nutritional deficiencies in coffee tree leaves through shape and texture descriptors. *J. Digit. Inf. Manag.* 15, 7–18.
- Wang, C., Ye, Y., Tian, Y., Yu, Z., 2021a. Classification of nutrient deficiency in rice based on CNN model with Reinforcement Learning augmentation. *Proceedings - 2021 International Symposium on Artificial Intelligence and its Application on Media*. 2021. ISAIAM, pp. 107–111. <https://doi.org/10.1109/ISAIAM53259.2021.00029>.
- Wang, Q., Mao, X., Jiang, X., Pei, D., Shao, X., 2021b. Digital image processing technology under backpropagation neural network and KMeans clustering algorithm on nitrogen utilization rate of Chinese cabbages. *PLoS One* 16, 1–24. <https://doi.org/10.1371/journal.pone.0248923>.
- Watchareeruetai, U., Noinongyao, P., Wattanapaiboonsuk, C., Khantiviriya, P., Duangsrissai, S., 2018. Identification of plant nutrient deficiencies using Convolutional Neural Networks. *IEEECON 2018-6th International Electrical Engineering Congress*, pp. 2018–2021. <https://doi.org/10.1109/IEEECON.2018.8712217>.
- Widodo, R., Widodo, A.W., Supriyanto, A., 2018. Pemanfaatan Ciri Gray Level Co-Occurrence Matrix (GLCM) Citra Buah Jeruk Keprok (*Citrus reticulata* Blanco) untuk Klasifikasi Mutu. *J. Pengemb. Teknol. Inform. Ilmu Komput.* 2, 5769–5776.
- Wulandhari, L.A., Gunawan, A.A.S., Qurania, A., Harsani, P., Triastinurmiatiningsih, Tarawan, Hermawan, R.F., 2019. Plant nutrient deficiency detection using deep convolutional neural network. *ICIC Expr. Lett.* 13, 971–977. <https://doi.org/10.24507/icicel.13.10.971>.
- Xu, Z., Guo, X., Zhu, A., He, X., Zhao, X., Han, Y., Subedi, R., 2020. Using deep convolutional neural networks for image-based diagnosis of nutrient deficiencies in rice. *Comput. Intell. Neurosci.* <https://doi.org/10.1155/2020/7307252>.
- Yan, X., Wen, L., Gao, L., Perez-Cisneros, M., 2019. A fast and effective image preprocessing method for hot round steel surface. *Math. Probl. Eng.* 2019. <https://doi.org/10.1155/2019/9457826>.